

# New $\text{Ni}_x\text{Mg}_{6-x}\text{MnO}_8$ Mixed Oxides as Active Materials for the Negative Electrode of Lithium-Ion Cells

R. Alcántara, M. Jaraba, P. Lavela, and J. L. Tirado<sup>1</sup>

Laboratorio de Química Inorgánica, Universidad de Córdoba, Edificio C3, planta 1, Campus de Rabanales, 14071 Córdoba, Spain

Received December 5, 2001; in revised form March 11, 2002; accepted March 22, 2002

New mixed oxides with an  $\text{Ni}_x\text{Mg}_{6-x}\text{MnO}_8$  ( $x = 0, 2, 4, 5$  and  $6$ ) stoichiometry and NaCl-related structure have been prepared by heating mixed oxalate precursors at  $600^\circ\text{C}$ . The existence of a solid solution was confirmed by the decrease of the cubic unit-cell parameter when magnesium was substituted by nickel. The solids were used as electrode materials in lithium cells, which were potentiostatically cycled. The structural transformations during reaction with lithium have been studied by *ex-situ* X-ray diffraction. A maximum value of ca.  $20 \text{ F mol}^{-1}$  is found during the first discharge of  $\text{Ni}_6\text{MnO}_8$  electrodes. Annealing the non-crystalline discharged electrodes at  $600^\circ\text{C}$  allows to detect metallic nickel. While  $\text{Ni}_5\text{MgMnO}_8$  improves capacity retention as compared with pure nickel, the extended substitution of nickel by magnesium leads to a progressive decrease in cell capacity. The reversible capacity values of  $\leq 640 \text{ mA h g}^{-1}$  are explained in terms of the formation of Ni oxide that reacts with lithium reversibly. The potential in which the cell current peaks occur decreases on increasing the Mg content. © 2002 Elsevier Science (USA)

**Key Words:** nickel; magnesium; manganese oxide; lithium-ion cells; electrochemical reaction; X-ray diffraction.

## INTRODUCTION

A new horizon of research has been opened in the domain of anodic materials for lithium-ion batteries. The reversible reduction of transition metal monoxides, such as those of cobalt, nickel and iron, to the zero oxidation state was recently described (1, 2) This electrochemical reaction is complex and must be accompanied, according to the authors, by the reversible formation of  $\text{Li}_2\text{O}$ . This conclusion is surprising and it has been always considered unlike in the great deal of papers on tin oxides in which  $\text{Li}_2\text{O}$  has been taken into account.

The structure of  $\text{Ni}_6\text{MnO}_8$  and  $\text{Mg}_6\text{MnO}_8$  has been previously reported in the literature (3, 4). Both solids have been described as a cubic closed packing of oxygen atoms

in which the metallic elements are octahedrally coordinated and cation vacancies are ordered in alternate (111) layers ( $Fm\bar{3}m$  space group). Hence, this framework can be considered as a distorted rock-salt-type structure.

The goal of this work is to study a new family of transition metal mixed oxides with the  $\text{Ni}_x\text{Mg}_{6-x}\text{MnO}_8$  ( $x = 0, 2, 4, 5$  and  $6$ ) general formula that reversibly react with lithium. The synthesis, characterization and electrochemical behavior as electrode materials in lithium batteries will be described. The occurrence of electrochemically active metal as nickel, and non-active metal as Mg is regarded as a way to shed new light on the parameters governing these electrochemical reactions.

## EXPERIMENTAL

The synthesis of the oxides was carried out by precipitation of mixed oxalates with  $\text{Ni}_x\text{Mg}_{6-x}\text{Mn}(\text{C}_2\text{O}_4)_7 \cdot 14\text{H}_2\text{O}$  to a nominal composition. Oxalic acid was added to an aqueous solution of the metal acetates and precipitated by heating to complete evaporation (4). Further heating of the precursors at  $600^\circ\text{C}$  in air for 3 h led to finely divided powders of oxide samples. The thermogravimetric (TG) curves of the precursors were recorded with a Cahn 2000 thermobalance in an air atmosphere.

X-ray powder diffraction (XRD) patterns were recorded on a Siemens D5000 instrument using  $\text{CuK}\alpha$  radiation and a graphite monochromator. After reaction with lithium, the samples for XRD were prepared inside a glove box (M Braun, containing less than 1 ppm  $\text{O}_2/\text{H}_2\text{O}$ ) by carefully opening the cells, placing the electrode material on a glass sample holder, and finally covering them with a plastic film to avoid exposure to air.

The electrochemical behaviour was tested in two-electrode Swagelok<sup>TM</sup> cells of the type  $\text{Li}|\text{LiPF}_6(\text{EC}:\text{DEC})|\text{Ni}_x\text{Mg}_{6-x}\text{MnO}_8$ . The oxide electrodes were prepared as 7 mm diameter pellets by pressing a mixture of 85% of the active material, 5% of PVDF binder and 10% carbon black to improve the mechanical and electronic conduction

<sup>1</sup>To whom correspondence should be addressed. Fax: +34-957-218621. E-mail: iqlticioj@uco.es.

properties, respectively. Lithium electrodes consisted of a clean 7 mm diameter lithium metal disk. The commercial electrolyte solution (Merck, 1 M LiPF<sub>6</sub> in a 1:1 w/w mixture of ethylene carbonate (EC) and diethylene carbonate (DEC)) was supported by porous Whatman glass-paper disks. The electrochemical measurements were performed by potentiostatic intermittent titration technique at 10 mV (0.1 h<sup>-1</sup>) rate, using a multichannel MacPile II system.

## RESULTS AND DISCUSSION

Five samples with a general composition of Ni<sub>x</sub>Mg<sub>6-x</sub>MnO<sub>8</sub> ( $x=0, 2, 4, 5,$  and  $6$ ) were obtained. The phase purity of the thermally treated oxalates was checked by XRD. The use of the precursor method allows us to reach an intimate mixture of the elements in the reagent which favors a homogeneous distribution of cations similar to that reported in the literature for the end Mg-free member of the series (3). In fact, oxalate precursors have been extensively examined in the past as precursors in the preparation of finely dispersed ferrites and other mixed spinel oxides (5). The simplicity of this low-temperature preparation method and the stability of the resulting products are obvious advantages over the preparation methods previously reported for other electrochemically active oxides.

### Thermogravimetric Study

In order to select the optimal annealing temperature, the TG curves of the oxalate precursors were recorded. The

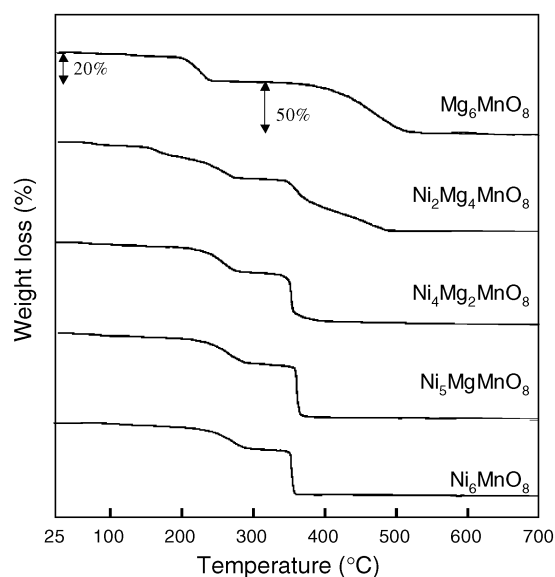


FIG. 1. Thermogravimetric curves of the oxalate precursors of Ni<sub>6-x</sub>Mg<sub>x</sub>MnO<sub>8</sub>.

data are shown in Fig. 1. Two main weight loss effects take place between room temperature and 700°C. The first one is located at ca. 250°C and accounts for ca. 20% of the initial weight in all samples. The second effect (about 50% of the initial weight) appears at a different temperature and with a different shape depending on the sample composition. In this way, the nickel-free precursor smoothly loses weight from ca. 450°C while the magnesium-free oxalate shows a steeper loss at ca. 350°C.

The first step can be unequivocally attributed to a dehydration of the oxalate precursor, as was checked by the stoichiometry of the hydrated and dehydrated of related products previously reported (3). On the other hand, the XRD profiles of the samples heated at the end of the second weight loss matches well with that of the oxide having the expected Ni<sub>x</sub>Mg<sub>6-x</sub>MnO<sub>8</sub> stoichiometries. According to these results, the precursors were annealed at 600°C for 3 h before the structural and electrochemical characterization.

### XRD Study

The XRD patterns of the oxide products are shown in Fig. 2. The patterns for the end members of these compounds were coincident with those reported in the literature (3, 4). They consist of a set of intense lines which are closely related to a rock-salt-type structure plus several smaller signals which arise from the superstructure caused by the ordering of the vacancies. The patterns corresponding to the intermediate compositions did not show

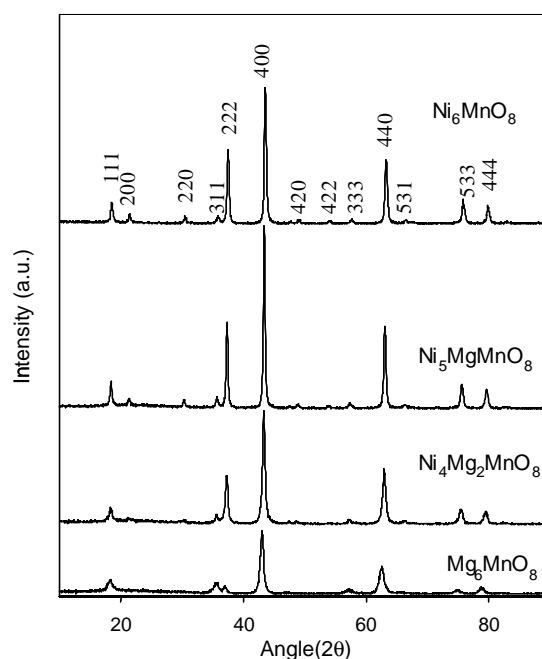


FIG. 2. XRD of the Ni<sub>6-x</sub>Mg<sub>x</sub>MnO<sub>8</sub> mixed oxides.

additional lines which could be assigned to the presence of impurities.

A poorer crystallinity can be observed as the magnesium content increases. This fact may be related with the higher decomposition temperature of magnesium-rich oxalates as was confirmed by the TG curves in Fig. 1. The annealing temperature used to prepare the oxides (600°C) is closer to the decomposition temperature for Mg-rich solids. As gaseous products are evolved during the decomposition of the oxalate precursor, a higher dispersion of the oxide diffracting domains is expected as nickel content decreases. The cubic lattice parameters were fitted by a squared minima routine according to the  $Fm3m$  space group (4). These results, plotted in Fig. 3, show a continuous decrease of the unit cell parameter with the nickel content, which is consistent with the smaller ionic radius of  $\text{Ni}^{2+}$  (0.69 Å) as compared with  $\text{Mg}^{2+}$  (0.72 Å), thus also indicating a homogenous cation distribution.

### Electrochemical Behavior

Figure 4 shows the voltage vs composition and current intensity vs voltage plots obtained by applying the PITT method to lithium cells using the  $\text{Ni}_x\text{Mg}_{6-x}\text{MnO}_8$  samples as active electrode material. As can be clearly observed, the substitution of nickel by magnesium involves a progressive loss of capacity whose minimum value corresponds to  $\text{Mg}_6\text{MnO}_8$ . Moreover, no reversible capacity for the first cycle was detected in this sample. Henceforth, magnesium can be considered in a first approach as an inert element in the electrochemical reaction of these compounds with lithium. A useful tool to elucidate possible reactions of active compounds in lithium cells is the use of thermodynamic parameters (6). Due to the lack of data from

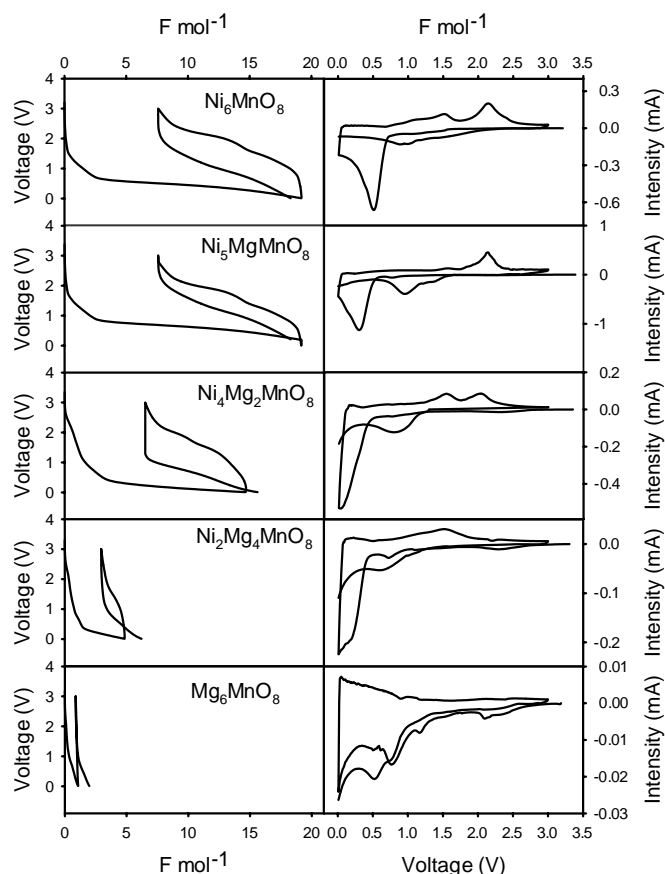
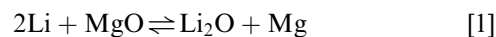


FIG. 4. Voltage vs composition and intensity vs voltage plots of  $\text{Ni}_{6-x}\text{Mg}_x\text{MnO}_8$  samples as obtained by the PITT method in lithium cells at  $10\text{ mV } (0.1\text{ h})^{-1}$ .

$\text{Ni}_6\text{MnO}_8$ ,  $\text{Mg}_6\text{MnO}_8$  or their solid solutions and taking into account the rock-salt-related structure of our oxides, we first considered the binary oxides of the elements present in these materials. Among the oxides potentially involved in our system, the value of Gibbs free energy of formation at 30 °C is more negative for  $\text{MgO}$  ( $-578.95\text{ kJ mol}^{-1}$ ) than for  $\text{Li}_2\text{O}$  ( $-561.20\text{ kJ mol}^{-1}$ ) (7), thus explaining that a reaction such as



is not thermodynamically allowed. On the contrary, the Gibbs free energy of formation of  $\text{NiO}$  ( $-216.57\text{ kJ mol}^{-1}$ ) is significantly less negative than that of  $\text{Li}_2\text{O}$ , as it was noticed in the first reports by Tarascon *et al.* (1, 2). Finally, in the case of  $\text{MnO}$  ( $-371.25\text{ kJ mol}^{-1}$ ) (7), the difference from  $\text{Li}_2\text{O}$  is not so marked, and the resulting potential should be closer to  $\text{Li}^+/\text{Li}$  than nickel or cobalt. In fact, in a recent report on  $\text{MnMoO}_4$ -based anodes Kim *et al.* (8) described that manganese was not reduced below  $\text{Mn}^{2+}$ .

The voltage vs composition curves are shown in Fig. 4. For all samples, the cell potential initially shows a steep

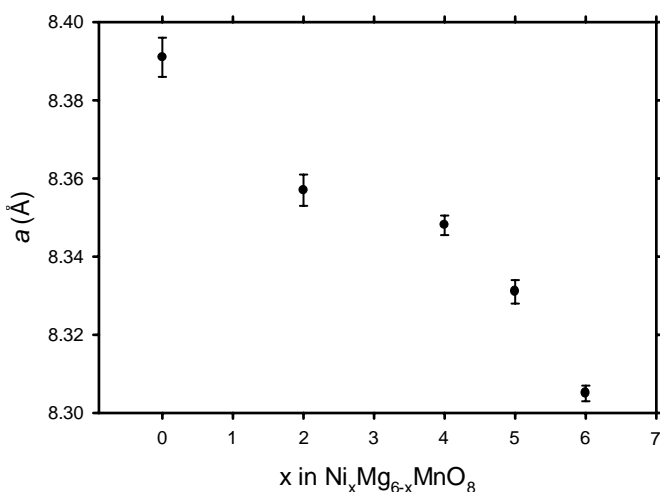
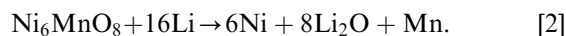


FIG. 3. Plot of the cubic unit cell parameter vs composition ( $x$ ) for  $\text{Ni}_{6-x}\text{Mg}_x\text{MnO}_8$ .

decrease leading to a quasi-plateau below 1.0 V. The length of this effect is proportional to the nickel content and takes values which agree fairly well with the extension of the Ni<sup>2+</sup>/Ni reduction, i.e., with the nickel content.

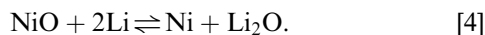
Extending the mechanism proposed by Tarascon *et al.* in binary oxides (1, 2) to our compounds, the first electrochemical reaction in the cells built up with Ni<sub>6</sub>MnO<sub>8</sub> anode material could be described as



Alternatively, the first discharge capacity could be due to the reduction to the metallic state of only nickel. Then the first discharge could be expressed as



In any case, the reversible charge/discharge cycles could be mainly expressed as:



In fact, a different cell potential is observed during the first and the second discharge in Fig. 4. This agrees well with a different reaction in the first discharge as compared with subsequent discharge branches. A similar behavior has been previously reported for other electrode materials, such as CoSb<sub>3</sub> (6), TiSb<sub>2</sub> (9) and CrSb<sub>2</sub> (10).

In reaction [3], MnO<sub>2</sub> was allowed to react in a limited extension with lithium having in mind that the initial Mn<sup>4+</sup> ions are effectively reactive toward lithium (11) and that Mn<sup>2+</sup> reduction is not easy (8). The electrochemical reaction of lithium with MnO<sub>2</sub> electrodes is a complicated process, and it has been the subject of several studies. Unfortunately, in most of the previous studies the working voltage was well above 0 V, and the discharged electrodes were difficult to characterize due to their degradation.

However, the observed capacity value for the first discharge of Ni<sub>6</sub>MnO<sub>8</sub> is higher than that expected even from Eq. [2], although the reversible capacity is lower and agrees well with Eq. [3]. As the metals are not alloying lithium, other possible reactions contributing to the total capacity of the first discharge may involve electrolyte decomposition. A possible small contribution of the carbon black additive should also be taken into account.

On the other hand, the detection of nickel in the discharged electrode could help to confirm the lithium reaction mechanism proposed. The XRD data recorded for the totally discharged and charged active material were characteristic of X-ray amorphous compounds (Fig. 5). Moreover, <sup>6</sup>Li RMN-MAS experiments of lithiated electrodes were not suitable because of the presence of ferromagnetic elements. In order to obtain more information about the lithiated samples, an Ni<sub>6</sub>MnO<sub>8</sub> electrode discharged down to 0 V was enclosed in a quartz tube while avoiding exposure to air by handling in a dry box, sealed under vacuum, and then heated at 600 °C for 2 days. The

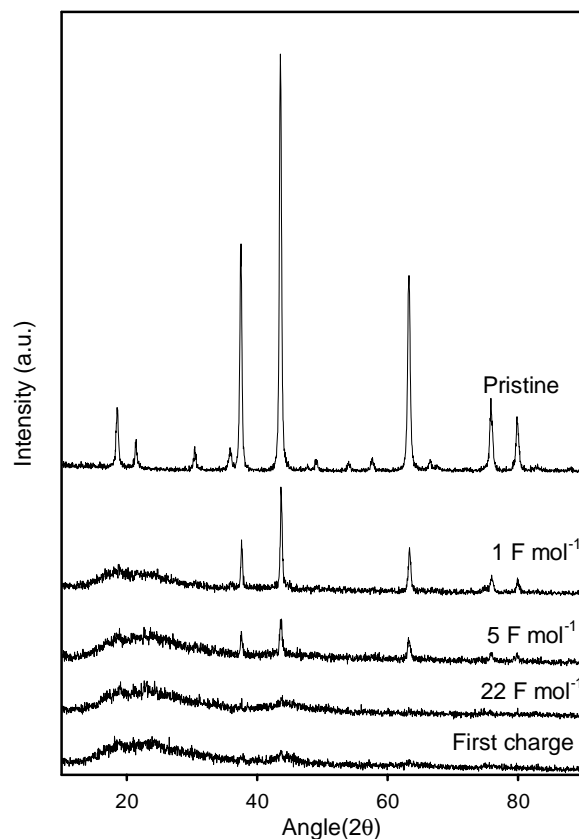


FIG. 5. X-ray diffraction pattern of pristine Ni<sub>6</sub>MnO<sub>8</sub> and corresponding electrodes at different depths of the first discharge, and charged up to 3 V.

XRD of this lithiated and annealed electrode is shown in Fig. 6. The increase in crystallinity by annealing allows the identification of the more intense reflections ascribable to Ni metal (marked with asterisks), Li<sub>2</sub>O and ramsdellite-related Li<sub>x</sub>MnO<sub>2</sub>. This is an indication of the fact that the reduction of nickel is the origin of the reversible reaction with lithium, as it is described in Eq. [3].

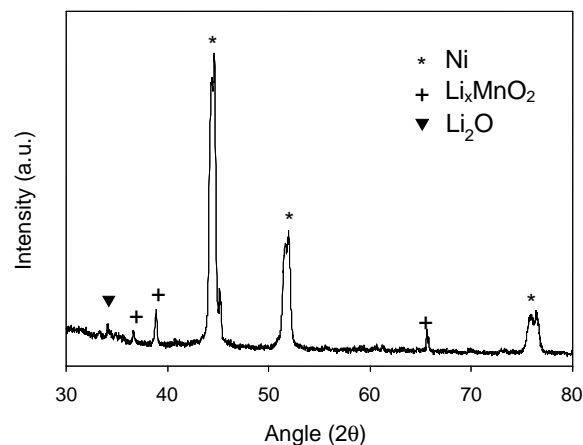
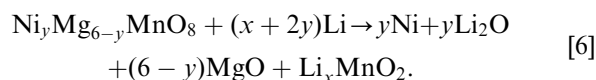


FIG. 6. *Ex-situ* XRD of an Ni<sub>6</sub>MnO<sub>8</sub> electrode discharged down to 0 V and then heated at 600 °C in a vacuum-sealed quartz tube for 2 days.

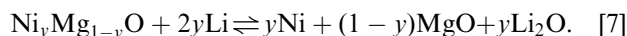
Additional complexity of the reaction results from the introduction of magnesium in the oxides. The intensity vs voltage plots (Fig. 4) show a continuous decrease in the extension of the voltage plateaus when the magnesium content increases. The possible contribution of the carbon black additive is probably the only factor responsible for the small capacity in  $\text{Mg}_6\text{MnO}_8$  cells. This behavior can be explained by taking into account the absence of Mg reduction and the Ni/Mg ratios in the studied compounds. In fact, for Mg-only sample the first discharge can be



The  $x$  value, which is common to Eq. [3], can be now derived from Fig. 4 to ca. 1. For intermediate compositions the first discharge is then



From Fig. 4, the potential in which the first-discharge quasi-plateaus develop decreases with the Mg content. This is most probably the complex result of different phenomena acting simultaneously, which include the mixing energy of an  $\text{Ni}_6\text{MnO}_8$ – $\text{Mg}_6\text{MnO}_8$  solid solution. For the second and subsequent charge/discharge branches, Eq. [4] can be modified to:



The full range of solubility between MgO and NiO is well known as a consequence of the fact that both binary oxides are face-centered cubic oxides with very close lattice parameters (12, 13). Thus, cycling voltage can also be affected by the mixing energy of the MgO–NiO solid solutions (12). Other effects include: (i) the PITT recordings are recorded under non-equilibrium conditions; (ii) once the first discharge has taken place and on subsequent cycle branches the element and oxide products are not thermodynamic standard forms, in fact all are X-ray amorphous, and (iii) the products are expected to be finely dispersed, which involves a non-negligible surface potential component. It should be noted that probably as a result of the combined effects, a significant reduction in cell polarization is obtained for  $\text{Ni}_5\text{MgMnO}_8$  electrodes.

The capacity retention of  $\text{Ni}_6\text{MnO}_8$  and  $\text{Ni}_5\text{MgMnO}_8$  for a few cycles are shown in Fig. 7 under different kinetic conditions of the potentiostatic measurements. Capacity retention and potential vs lithium are the major limitations to overcome in the application of these materials. Capacity values higher than  $400 \text{ mA h g}^{-1}$  were kept after 10 cycles for both samples at rates as high as  $50 \text{ mV} (0.1 \text{ h}^{-1})$ . However, a better charge retention was detected for  $\text{Ni}_5\text{MgMnO}_8$ . An additional experiment was made in which cycling rate was significantly reduced. Under these conditions, the cell built by using  $\text{Ni}_5\text{MgMnO}_8$  as the working electrode achieved capacity values higher than

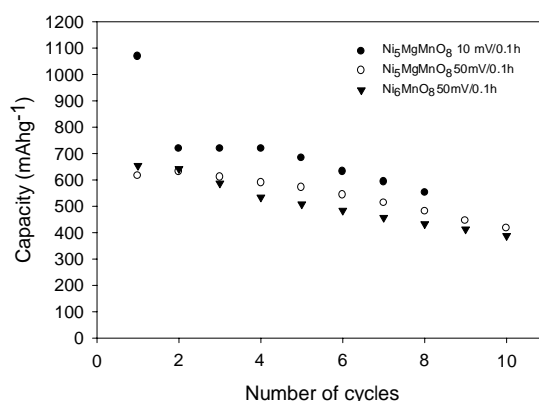


FIG. 7. Cell capacity vs. cycle number of  $\text{Li/LiPF}_6/\text{Ni}_{6-x}\text{Mg}_x\text{MnO}_8$  cells.

$550 \text{ mA h g}^{-1}$  after eight cycles. The role of low contents of magnesium on this effect is not clear. At this point, it should be noted that the advantages of MgO/NiO solid solutions as referred to pure NiO have also been reported in catalysis. It has been shown that it is more difficult to reduce the NiO to Ni in a solid solution and that the resulting Ni is highly dispersed (13). This, in turn, is interesting in order to avoid extensive metal clustering that could result in a loss of capacity on prolonged cycling, as found in Sn compounds (14).

## CONCLUSIONS

New  $\text{Ni}_{6-x}\text{Mg}_x\text{MnO}_8$  mixed oxides have been obtained, and it has been shown that these materials are able of reacting reversibly with lithium. These oxides are inexpensive, and easy to prepare even at low temperatures by thermal decomposition of oxalate precursors. Using them as electrodes in lithium batteries reversible capacities are about  $700 \text{ mA h g}^{-1}$ . The reaction with lithium takes place through the reduction of the transition metal ions and an amorphization process. The presence of a small amount of magnesium has certain advantages such as reducing cell polarization and facilitating Ni dispersion, which in turn improves capacity retention.

## ACKNOWLEDGMENTS

The authors acknowledge the financial support from CICYT (Contracts MAT99-0741 and MAT2000-2721-CE).

## REFERENCES

1. P. Poizot, S. Laruelle, S. Grugeon, L. Dupont, and J. M. Tarascon, *Nature* **407**, 496–499 (2000).

2. P. Poizot, S. Laruelle, S. Grugeon, L. Dupont, B. Beaudoin, and J. M. Tarascon, *C. R. Acad. Sci. Paris, Sér. IIC, Chem.* **3**, 681–691 (2000).
3. A. Feltz and J. Töpfer, *J. Alloys Compds.* **196**, 75–79 (1993).
4. P. Porta, G. Minelli, I. L. Botto, and E. J. Baran, *J. Solid State Chem.* **92**, 202–207 (1991).
5. M. Paulus, in “Preparative methods in Solid State Chemistry” (P. Hagenmuller, Ed.), p. 506, Academic Press, New York, 1972.
6. R. Alcántara, F. J. Fernández Madrigal, P. Lavela, J. L. Tirado, J. C. Jumas, and J. Olivier-Fourcade, *J. Mater. Chem.* **9**, 2517–2521 (1999).
7. C. B. Alcock, “Handbook of Chemistry and Physics,” p. 5–72 to 5–75. CRC Press, New York, 1993.
8. S. S. Kim, S. Ogura, H. Ikuta, Y. Uchimoto, and M. Wakihara, *Solid State Ion.* **146**, 249 (2001).
9. D. Larcher, L. Y. Beaulieu, O. Mao, A. E. George, and J. R. Dahn, *J. Electrochem. Soc.* **147**, 1703–1708 (2000).
10. F. J. Fernández-Madrigal, P. Lavela, C. Pérez-Vicente, and J. L. Tirado, *J. Electroanal. Chem.* **501**, 205–209 (2001).
11. M. M. Thackeray, *Prog. Solid State Chem.* **25**, 1–71 (1997).
12. K. D. Heath, W. C. Mackrodt, V. R. Saunders, and M. Causà, *J. Mater. Chem.* **4**, 825–829 (1994).
13. Y. H. Hu and E. Ruckenstein, *J. Catal.* **184**, 298–302 (1999).
14. I. A. Courtney, W. R. McKinnon, and J. R. Dahn, *J. Electrochem. Soc.* **146**, 59–68 (1999).